Advances in Water Resources 205 (2025) 105071

Contents lists available at ScienceDirect

Advances in Water Resources

journal homepage: www.elsevier.com/locate/advwatres

Non-stationary frequency analysis of long-term convection permitting simulations reveals sub-daily extreme precipitation changes in central-southern Europe

Marco Lompi [a,*], Francesco Marra [b], Roberto Deidda [c], Enrica Caporali [a], Marco Borga [d], Eleonora Dallan [d]

[a] Department of Civil and Environmental Engineering, University of Florence, Italy
[b] Department of Geosciences, University of Padova, Italy
[c] Department of Civil, Environmental and Architecture Engineering, University of Cagliari, Italy
[d] Department of Land, Environment, Agriculture and Forestry, University of Padova, Italy

ARTICLE INFO

Keywords:
Extreme precipitation
Climate change
Convection permitting model
Non-stationary frequency analysis
Mediterranean climate

ABSTRACT

Assessing the impact of climate change on extreme precipitation is a critical task for adapting flood mitigation strategies. Nowadays, Convection Permitting Models (CPM) are the state-of-the-art tool to simulate current and future extreme precipitation, as they explicitly represent convective processes, outperforming climate models with coarser resolutions. Nevertheless, CPM are computationally demanding and typically limited to decadal periods, making them potentially more affected by internal variability.

Here, we exploit for the first time long-term CPM simulations over Central-Southern Europe to develop a non-stationary analysis of extreme precipitation. We use VHR-PRO_IT (Very High-Resolution PROjections over Italy), recent CPM projections with high spatiotemporal resolution (2.2 km and 1 h) and simulations spanning 90 years in two emission scenarios. We apply a non-asymptotic statistical approach (SMEV) with a non-stationary implementation using time as a covariate. This approach allows us to capture the transient change in precipitation extremes and in their distribution parameters, describing trends beyond the natural variability, which could affect short (decadal) simulations.

We find a general increase of sub-daily extreme precipitation in a warmer climate, especially in the Mediterranean areas. Larger areas with statistically significant changes are found at shorter durations. Higher increases are expected with higher return periods (median value of about 3–4 % / decade at 100 yr return period), especially for longer durations. This can be explained by the increasing distribution tail heaviness found at those durations. Average expected changes in extreme precipitation are similar in the two scenarios, but larger non-stationary areas are expected in the RCP8.5.

1. Introduction

Extreme rainfall contributes to natural disasters that cause enormous human and economic damage (Munich RE, 2023). Numerous studies have examined the impact of climate change on the frequency and intensity of extreme precipitation in both models and observations, consistently reporting projected increases across nearly all global land areas (Donat et al., 2016; Li et al., 2019; Martel et al., 2021; Prein et al., 2017; Papalexiou and Montanari, 2019). These findings align with the theoretical understanding of the underlying physical processes, as higher atmospheric temperature implies higher potential amounts of water vapor available for extreme precipitation (Marra et al., 2022; Sevinaratne et al., 2021; Zhang et al., 2024). A quantification of future changes in extreme precipitation is crucial to support policy decisions for land management or infrastructure design (e.g. Lompi et al., 2023) and investments in flood defences for adapting to a future climate (IPCC, 2022).

Future changes in extreme precipitation are usually assessed based on climate projections from Regional Climate Models (RCM), which dynamically downscale the results of the Global Climate Models (GCM)

* Corresponding author: Via di Santa Marta 3, Firenze 50139, Italy.
E-mail address: marco.lompi@unifi.it (M. Lompi).

https://doi.org/10.1016/j.advwatres.2025.105071
Received 28 March 2025; Received in revised form 1 August 2025; Accepted 2 August 2025
Available online 5 August 2025
0309-1708/

to resolutions on the order of 10 km. Despite continuous improvements, RCMs still struggle to realistically represent extreme precipitation because their resolution is insufficient to explicitly resolve convection - a fundamental process driving the most intense precipitation, particularly at sub-daily scales. Additionally, their coarser resolution also hinders the accuracy in representing topography and coastlines, which are important factors that influence extreme precipitation. Convection Permitting Models (CPMs), which operate at finer resolutions ($\leq$ 4 km), explicitly resolve deep convection, eliminating the need for its parametrization (Luchas-Picher et al., 2021; Prein et al., 2015). As a result, CPMs provide more accurate simulation of extreme precipitation events (Ban et al., 2014, 2021; Luu et al., 2022; Pichelli et al., 2021) and have proved advantages in capturing sub-daily extreme precipitation across various climate conditions (Fosser et al., 2020, 2024; Kendon et al., 2014; Meredith et al., 2020).

Owing to their high computational costs, CPM simulations are often provided as short time slices, typically on the order of 10–20 years at most (Cannon and Innocenti 2019). For this reason, only a limited number of studies investigated the changes in extreme precipitation simulated by CPM in terms of rare annual exceedance probabilities (or their inverse, return periods), the metric commonly used in hydrological and engineering applications (Ban et al., 2020; Chan et al., 2023; Dallan et al., 2024a,b).

However, in very recent years, a few long (70–100-year) convection-permitting projections have been developed (Kendon et al., 2023; Raffa et al., 2023), opening new perspectives on estimating rare precipitation return levels under transient climatic conditions. Utilizing a 100-year CPM simulation ensemble over the UK, Kendon et al. (2023) demonstrated that internal variability can lead to years with record-breaking extreme events followed by multiple decades with no new local rainfall records, potentially affecting results based on decadal-long CPM simulations. This clustering of extreme years presents significant challenges for communities trying to adapt. However, when precipitation return levels are used for design purposes, the focus must shift to long-term trends. In this context, non-stationary statistical models can be employed.

A few studies have explored the possible presence of trends in the future extreme sub-daily precipitation using non-stationary analysis of climate model simulations, generally using coarse resolution models. Rashid et al. (2017) developed non-stationary models of future extreme rainfall using reanalysis datasets and outputs from General Circulation Models (GCMs) as covariates. Lee et al. (2020) used a non-stationary peak-over-threshold method to derive rainfall extremes from GCM temperature projections, identifying a consistent rate of change across models. Silva et al. (2021) used a non-stationary Generalized Extreme Value distribution with time-dependent parameters to provide a more dynamic understanding of extreme precipitation changes. Also Seo et al. (2021) analyzed future extreme rainfall using a similar model by incorporating future surface air temperature and dew point temperature as covariates, which significantly helped in reducing uncertainties associated with the projections. Moreover, Sojan et al. (2023) applied the same approach to GCM projections over Asia, identifying regions with less variability in future extreme rainfall while highlighting an increase in the frequency of high-magnitude events.

Despite these advancements, non-stationary applications of extreme value theory typically rely only on annual maxima (or a limited number of peaks exceeding a high threshold). As a result, they utilize only a fraction of the available climate projection data, leading to significant estimation uncertainties that often obscure climate change signals (e.g., see Dallan et al., 2024a). Due to parameter estimation uncertainty, some model parameters (often two out of three) are typically held constant, while only one or a few are allowed to depend on the covariate of interest. Since these parameters are not independent, such constraints can introduce biases in precipitation estimates and lead to inconsistent model specifications (Prosdocimi and Kjeldsen, 2021). This underscores the need for improved non-stationary precipitation frequency analyses that can provide more reliable estimates of future extreme precipitation. To overcome these limitations, recent advancements in the statistical analysis of extremes based on ordinary values, such as the Metastatistical Extreme Value (MEV) method (Marani and Ignaccolo, 2015) and its simplified implementation (SMEV) (Marra et al., 2019), may offer a possible alternative. At the price of using different assumptions with respect to the extreme value theorem, these methods provide more reliable estimates of extreme events with low exceedance probabilities, even from relatively short time series. This is done by incorporating a large set of ordinary events in the statistical inference, instead of relying solely on annual maxima or peaks above a high threshold (e.g., see Dallan et al., 2024a,b; Zorzetto et al., 2016). Also, their formulation separates the yearly occurrence of events and the intensity distribution, allowing a physical interpretation of the statistical results (e.g., Amponsah et al. 2022; Dallan et al., 2022, 2024a,b; Formetta at al. 2022; Hosseini et al., 2020; Miniussi et al., 2020a,b). In the context of non-stationary implementation of these methods, Vidrio-Sahagún & He (2022) compared non-stationary MEV, SMEV and GEV models to assess their fitting efficiency, showing that SMEV-based models have higher accuracy and lower uncertainty.

This study aims to assess the transient changes in sub-daily precipitation extremes across the central-southern Europe region under two emission scenarios, leveraging the longest CPM simulations currently available for the region. The projections used are VHR-PRO_IT, Very High Resolution PROjections over ITaly (Raffa et al., 2023), a dynamical downscaling of the CMCC—CM global model at a convection-permitting scale of 2.2 km, with outputs at 1 h temporal resolution. To date, this is the only CPM projection available under both emission scenarios (RCP 4.5 and RCP 8.5) over a 90-year period (1981–2070; 1981–2005 historical + 2006–2070 projections). To achieve this, we employ a non-stationary implementation of the Simplified Metastatistical Extreme Value (SMEV) approach (Marra et al., 2019), which significantly mitigates parameter estimation uncertainties and allows to exploit the information from the 90-year simulation for analyzing both the changes in precipitation quantiles at high return periods and the changes in their distribution parameters. This is achieved through a reduced number of parameters, a larger sample size used for parameterization, and the possibility to tailor the model to the tail of the precipitation distribution predicted by atmospheric physics (Marra et al., 2020; Wilson and Toumi, 2005). To the best of our knowledge, this study represents the first application of non-stationary frequency analysis to multi-decadal convection-permitting climate models.

2. Data & study area

The domain of VHR-PRO_IT is illustrated alongside the Digital Elevation Model of the climate model in Fig. 1. The analysed area covers the centre south of Europe with many different climate conditions and orography, and it includes Italy, Switzerland, Austria, Slovenia, Croatia, Bosnia and parts of France, Germany, the Czech Republic, Slovakia, Hungary and Montenegro.

A comprehensive extreme precipitation climatology of the area is reported in Avanzi et al. (2015) and Poschlod et al. (2021). In particular, the maps reported by Poschlod et al. (2021) show that the ten-year return levels span between 17 and 40 mm for one hour and between 40 and 220 mm for 24 h. These maps, combined with those from Avanzi et al. (2015) highlight that the highest quantiles at hourly duration occur along most of the coastlines, with particularly high values observed in southern Friuli–Venezia Giulia, the Mediterranean coast areas of France, western coast of central Italy, and the eastern coasts of Sicily, Calabria, and Sardinia. Furthermore, high values of ten-year hourly quantiles are found across the Po Valley. As the duration increases from 1 hour to 24 h, the areas characterised by high return levels become more localized. These areas include the northwestern Alps, the Mediterranean coast of France, western Italian coasts, eastern Sardinia, Friuli–Venezia Giulia, southern Calabria, and eastern Sicily. This

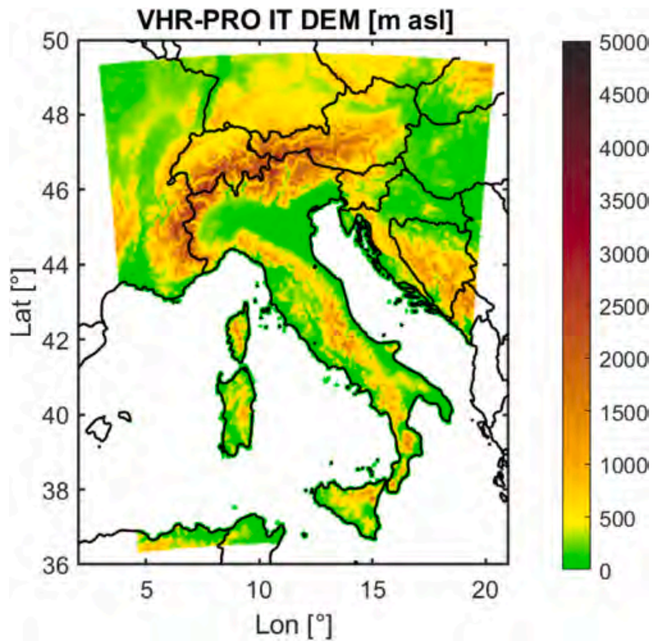

Fig. 1. Elevation in the case study area (m asl) in the VHR-PRO_IT domain. The area includes Italy, Switzerland, Austria, Slovenia, Croatia and Bosnia, while also partially extending into eastern France, southern Germany, the Czech Republic, western Slovakia, Hungary, and Montenegro.

transition in the spatial extent of extreme precipitation suggests a shift in dominant precipitation mechanisms: 1-hour extremes are typically associated with convective storms, whereas 24-hour extremes are typically associated with mixed processes, including both convective and stratiform precipitation (e.g., Formetta et al., 2022). Recent studies on observed precipitation trends in Italy show an increase of precipitation intensity (Caporali et al., 2021), with stronger changes in the more extreme events with respect to lower quantiles in many areas (Mazzoglio et al., 2025a). These results have especially been detected for short durations (1 h), while some negative trends in longer durations (24 h) are also observed.

VHR-PRO_IT (Raffa et al., 2023) is a dynamical downscaling of the CMCC—CM Global Climate model at a convection-permitting scale of 2.2 km, with an intermediate nesting at a spatial resolution of 8 km. The downscaling has been performed with the COSMO—CLM model, and the precipitation values are provided with an hourly temporal resolution. In this work, we analyse the whole domain of VHR-PRO_IT, which was released after removing the outermost grid cells from the original computational domain of 620 × 692 points, resulting in a refined domain of 570 × 652 points to minimize boundary effects. To date, this is the only CPM projection over a wide region, including all of Italy and the entire Great Alpine area, under two emission scenarios (RCP 4.5 and RCP 8.5) and over a 90-year period (1981–2070). VHR-PRO_IT shows overall reliable performance, with temperature and precipitation biases generally consistent with those of the Euro-CORDEX models. Particularly, the historical period of the projections shows an underestimation of the temperatures, an overestimation of precipitation in the northern part of Italy and an underestimation in the center and south (Raffa et al., 2023), as in many models of the Euro-CORDEX. Future changes in the 99.9th hourly percentile of precipitation were found consistent with the spread of the multi-model CPM ensemble in Pichelli et al. 2021 (Raffa et al. 2023).

The accuracy of these simulations in reproducing precipitation properties over Italy has been assessed by Mazzoglio et al. (2025b) through a systematic comparison with rain gauge observations from I2-RED, a comprehensive dataset of yearly maxima at daily and sub-daily durations recorded by >5000 quality-checked rain gauge stations (Mazzoglio et al., 2020). The comparison between simulations and observations was performed by considering two steps. Firstly, the medians of the distribution of annual maxima were compared to explain the control of certain geographical features on CPM biases. Second, medium-to-high return period rainfall quantiles, which are particularly relevant for hydrological design, were considered. Both the comparisons highlighted that VHR-PRO_IT provides satisfactory results when considering longer duration events (6 to 24 h), while shorter durations (1 and 3 h) are affected by underestimations, especially in coastal and low-elevation areas. The underestimation increases when moving southward along Italy. On the contrary, rainfall quantiles from VHR-PRO_IT compare satisfactorily with observations at medium-to-high elevations, over inland areas and in the Northern part of the country. These results broadly agree with those obtained by Raffa et al. (2023) in a comparison of heavy hourly precipitation (i.e., the 99.9th percentile of all events) for Northern, Central and Southern Italy with the hourly gridded dataset GRIPHO relying on the interpolation of data from local weather stations at ~10 km. The comparison showed negative biases increasing from Northern (−5 %) to Southern Italy (−25 %).

Results from Raffa et al. (2023) on the future changes for 2050 show that changes in heavy hourly precipitation are mainly related to the analysed scenario. For RCP 8.5, an increase is reported for Northern Italy (3,5 %), whereas a decrease is reported for Southern Italy (−6 %). The RCP 4.5 scenario shows a reduction for the three regions, with a decrease more pronounced in Southern Italy (−25 %).

3. Methodology

We use a non-stationary implementation of the Simplified Meta-statistical Extreme Value (SMEV) approach (Marra et al., 2019), an approach developed from the ideas first proposed by Marani and Ignaccolo (2015). Thanks to its structure, SMEV can be effectively tailored to the specific characteristics of the available data. In particular, the implementation proposed by Marra et al. (2020) enables a consistent evaluation of different sub-daily durations. With SMEV, we isolate independent storms as wet periods separated by dry intermissions of at least 24 h, as recommended in Marra et al. (2020), and we define the ordinary events of a duration of interest as the maximum intensity observed in each storm over moving windows of the given duration. Following Wilson and Toumi (2005), we use a two-parameter Weibull distribution to describe the tail behavior of the cumulative distribution F of the ordinary events. Using n to represent the average annual number of storms (and hence, also of ordinary events of any duration), the distribution of annual maxima can be approximated as follows (Marra et al., 2019):

$$SMEV(x) = [F(x;\boldsymbol{\theta})]^n \text{ with } F(x;\boldsymbol{\theta}) = F(x;\lambda,\kappa) = 1 - e^{-\left(\frac{x}{\lambda}\right)^{\kappa}} \tag{1}$$

where x describes the maximum precipitation of a fixed duration (see Marra et al., 2020), while λ and κ are, respectively, the scale and shape parameters of the Weibull distribution. Higher shape parameters correspond to lighter-tailed distributions and vice versa (see the example for the extreme rainfall in 1 h duration in Figure 1S in the Supplementary Material).

We use time as a covariate of our non-stationary model. While physics-based covariates (such as temperature) can be more useful from the perspective of process understanding and future projections (e.g., Martel et al., 2021), here we are interested in describing the changes in extremes over a long period with a transient climate. Analysing such a long period makes it difficult to select a physical covariate properly because, in reality, several covariates contribute to shaping extremes, and their relative importance may not remain constant. For example, the most used physical covariate, temperature, mostly explains changes in the thermodynamics of the atmosphere, but cannot well represent the expected modifications of large-scale atmospheric dynamics (e.g., see Marra et al., 2024). The separation of intensity distribution and number of events in SMEV structure allows us to infer potential physical mechanisms behind such observations, by using the approach in Dallan et al. (2024a,b). Indeed, the non-asymptotic approach allows the discussion of the results in terms of changes in the scale parameters, which are more likely linked with thermodynamic drivers, and changes in the shape parameter that can be associated with variations in the dynamic drivers.

The analysis has been divided into two phases. In the first phase, a stationary SMEV model (i.e., with parameters constant over time) is applied with a moving window of 30 years to qualitatively evaluate the dependence of the model parameters on time. More specifically, the analysis is carried out to assess whether a simple hypothesis of linear dependence of the parameters on time is clearly rejected by the data. To account for estimation uncertainty, we replicated the estimates at each 30-year window using a bootstrap with replacement (Overeem et al., 2008). We randomly sampled 30 years out of 30 to create 100 surrogate time series and replicated the estimates for each series. The analysis has been conducted on a sample of representative sites to investigate the extreme storm climatology in the study domain. The results of this preliminary analysis suggest that a linear dependence of the SMEV parameters over time is a reasonable assumption (see more details in the Supplementary Material from Figure 2S to 8S) .

In the second phase, a non-stationary implementation of the SMEV is used to evaluate changes in precipitation quantiles for return periods from 2 years to 100 years, for different durations (1 hour, 3, 6, 12 and 24 h) over the period 1981–2070 (historical 1981–2005 + future scenarios 2006–2070). According to the results of the first phase, i.e. a linear dependence of the SMEV parameters over time as a reasonable assumption, three different models are compared in the second phase to assess the possible presence of significant trends in one or both the distribution parameters: i) a stationary SMEV, with the two parameters constant over time (Eq. (1)); ii) a partial non-stationary SMEV model in which the shape parameter held constant and the scale parameter is allowed to change linearly with time (Eq. (2));

$$SMEV(x) = [F(x;\lambda(t),\kappa)]^n \text{ with } F(x;\lambda(t),\kappa) = 1 - e^{-\left(\frac{x}{\lambda_1+\lambda_2 t}\right)^{\kappa}} \tag{2}$$

iii) a fully non-stationary SMEV model where both parameters are allowed to change linearly with time (Eq. (3)).

$$SMEV(x) = [F(x;\lambda(t),\kappa(t))]^n \text{ with } F(x;\lambda(t),\kappa(t)) = 1 - e^{-\left(\frac{x}{\lambda_1+\lambda_2 t}\right)^{\kappa_1+\kappa_2 t}} \tag{3}$$

Where λ_1, λ_2 are respectively the intercept and the slope in the linear dependence of the scale parameter over time, while κ_1, κ_2 have similar roles in modelling possible changes of the shape parameter with time. The possible dependence of the average annual number of events n on time has not been tested due to the low sensitivity of extreme quantiles to the average annual number of ordinary events n (see the appendix A in Siena et al., 2023).

The likelihood ratio test is used to evaluate the statistical significance of the time dependence of the parameters. Therefore, the possible presence of statistically significant changes in the precipitation distributions is tested by evaluating the statistical significance of the differences between the likelihoods evaluated with constant parameter models (Eq. (1), null hypothesis) and the likelihoods with models that have scale (Eq. (2)) and possibly shape (Eq. (3)) parameters varying over time, as in Coles (2001). The use of the different SMEV models and the log-likelihood ratio test is important for identifying the trends in the parameter distributions and to link extreme precipitation changes to possible drivers. Indeed, this non-asymptotic approach allows the discussion of the results in terms of dynamic and thermodynamic drivers. The changes in the scale parameter alone are more likely linked with thermodynamic drivers, whereas changes in the shape parameter can be associated with variations in the dynamic drivers (E. Dallan et al., 2024b).

In both phases, the maximum likelihood approach with left-censoring is used to estimate the parameters (codes freely available from Marra, 2025). The choice of threshold in the left-censoring approach (i.e., considering the values below a chosen threshold as non-exceedances instead of exact values) is crucial to match the theoretical results from Wilson and Toumi (2005). Nevertheless, to have homogeneous results and comparable uncertainty across the entire domain (essential to assess the statistical significance homogeneously), the choice of a common threshold for the entire study area is necessary. In this study, we used 0.8 based on the results from Dallan et al. (2023) and Marra et al. (2022). Dallan et al. (2023) identified the best thresholds for northeastern Italy as 0.9 for the duration of 1 h and 0.85 for all the others, while Marra et al. (2019) used a threshold of 0.75 in semiarid and arid regions of the eastern Mediterranean. Our choice may lead to biases in some areas, but the setup of the study in which changes are expressed in relative terms (see below) is expected to minimize the potential impact of such biases.

Maps with expected trends of the SMEV parameters are presented by showing λ_2 and κ_2, i.e. the slope of the corresponding parameters over time. As summary statistics, we computed the spatial-average relative changes of each parameter per decade (10 years), normalized by its value at the beginning of the period, λ_1 and κ_1, as in the following equations.

$$\Delta\lambda(\%) = \frac{\lambda_2 * 10y}{\lambda_1} * 100 \tag{4}$$

$$\Delta\kappa(\%) = \frac{\kappa_2 * 10y}{\kappa_1} * 100 \tag{5}$$

Since linear variations of SMEV parameters are not reflected in linear variations of quantiles, changes in the extreme precipitation are derived with reference to the 90 years of the VHR-PRO_IT simulations but shown as relative changes per decade for given quantile q and duration d as:

$$\Delta P_{q,d}(\%/decade) = \frac{P_{q,d,2070} - P_{q,d,1981}}{P_{q,d,1981}} * \frac{100}{9} \tag{6}$$

Since the analysis is conducted cell by cell, a 3 × 3 spatial filter is used to smooth and remove noise in the obtained results (e.g., Panziera et al., 2016).

4. Results

This section has the following structure: first, the changes in the parameters and their statistical significance are presented to highlight the areas where changes in extreme precipitation are statistically significant (Section 4.1); then, expected changes in extreme precipitation are shown (Section 4.2). Maps with expected changes in the parameters and the extreme precipitation are shown in this section for the RCP 8.5 scenario and three storm durations (1 h, 6 h, 24 h), while spatial average changes are given for all the scenarios. Maps for the other durations (3 h and 12 h) and the RCP 4.5 are provided in the Supplementary Material.

4.1. Expected changes in the SMEV parameters

Fig. 2 shows the results of the likelihood ratio tests for the three considered durations, using as a null hypothesis a stationary distribution of maximum rainfall (according to Eq. (1)) with a level of significance of 5 %. Areas characterized by statistically significant changes in the scale parameter only are depicted in cyan, while areas where significant changes in both scale and shape parameters are marked in blue.

In the white areas, the null hypothesis of a stationary model cannot be rejected. In general, the partial non-stationary model (i.e. varying scale with time and constant shape parameter, see Eq. (2)) seems to

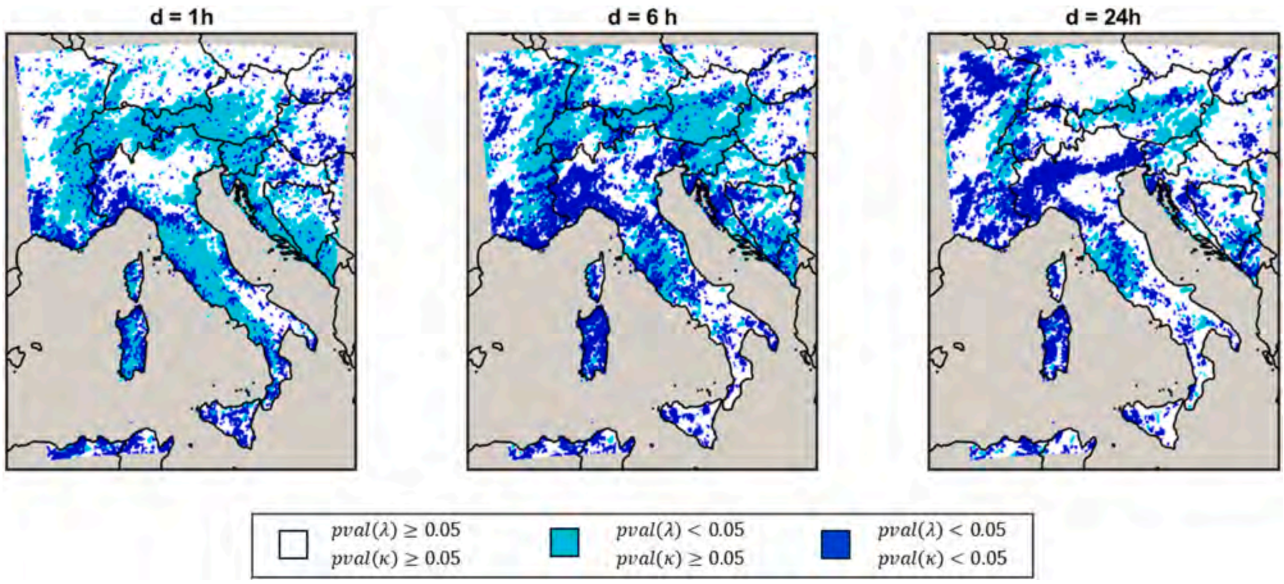

Fig. 2. Results of the likelihood ratio test for the RCP 8.5 scenario: the areas in cyan have significant trends (p-value <0.05) in the scale parameter; the blue ones have significant trends in both the scale and shape parameters. The null hypothesis of a stationary distribution was not rejected for the white areas. Grey areas represent the Mediterranean Sea or regions outside the VHR-PRO_IT domain.

prevail at 1 h duration, especially in the Great Alpine area and central Italy. In contrast, the fully non-stationary model (Eq. (3)) appears to be more relevant for durations longer than or equal to 6 h, especially in northwestern Italy and the island of Sardinia. For longer durations, a stationary model could be used for the northern part of the domain and generally along eastern and southern Italy. The areas with statistically significant trends in the RCP 4.5 are smaller (Figure 9S in the Supplementary Material), with the exception of significant changes in the scale

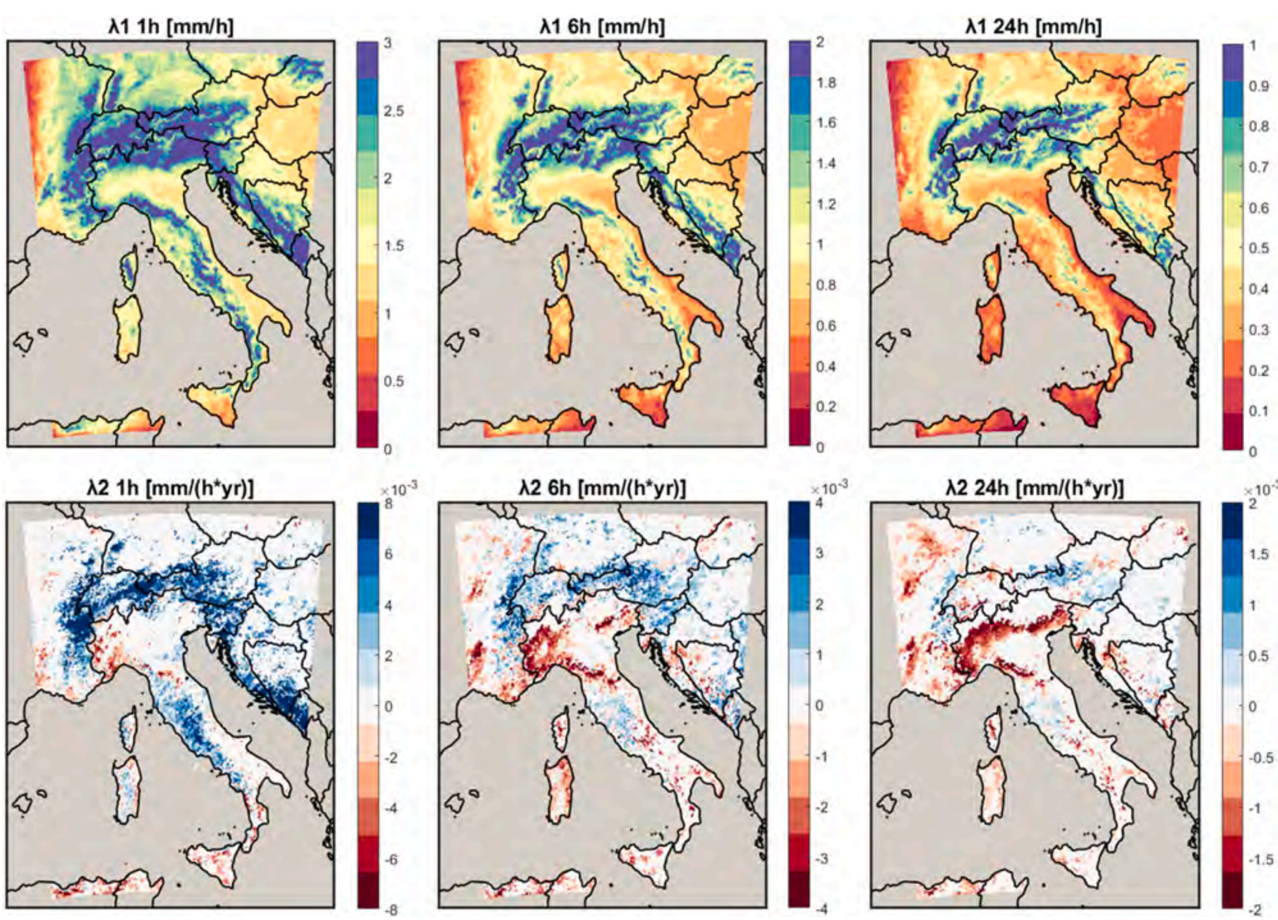

Fig. 3. Spatial map of λ_1, scale parameter at the beginning of the time series (1981), and $\lambda_2$its slope in the linear dependence over time for the RCP8.5 scenario. Grey areas represent the Mediterranean Sea or regions outside the VHR-PRO_IT domain.

parameter for short durations in Germany, which are not present in the RCP 8.5.

Fig. 2 shows the areas where the trends are significant without giving any information about the direction of the trend. Figs. 3 and 4 show the initial values and the trends in the distribution parameters obtained using the fully non-stationary model (Eq. (3)). The rationale behind examining the results of the full non-stationary model is that Dallan et al. (2022) showed that changes in the shape parameter can sometimes be not statistically significant by themselves, and yet remain the only possible explanation of the observed patterns of significant change in the quantiles.

In the lower subplots of Figs. 3 and 4, areas where the stationary model cannot be rejected are marked in white, while areas with statistically significant increasing (decreasing) changes in the parameters are coloured in blue (red).

Subplots in the first row of Fig. 3 show the maps of λ_1 estimates, i.e. the scale parameter at the beginning of the time series (1981) for the three durations. We can observe a similar spatial pattern across all considered durations, with greater values in the mountainous zones: in the Alps (Italy, Switzerland, and Austria), the Apennines (central Italy), and along the Dinaric Alps (Slovenia, Croatia, and Bosnia). Indeed, even if several factors can influence extreme precipitation (such as exposure or proximity to the sea), zones with higher altitude often experience a larger variability and higher intensity in extreme precipitation events (higher scale), due to orographic effects and more variable local atmospheric conditions. Despite the original border cut of the VHR-PRO_IT computational domain (see Section 2), some boundary effects may still be visible in the Southern and Western grid points, where parameter estimates result in smaller values. Maps of λ_2, i.e. the estimated slope (per year) of the scale parameter, are plotted in the lower subplots of Fig. 3 for the same durations. The scale parameter is projected to increase, especially for short durations, in the Great Alpine area, the coastal region of the eastern part of the domain, and central-eastern Italy. Positive trends in the scale parameter are detected especially for 1h-duration, and this could be associated with an expected increase in precipitation quantiles for short durations due to more intense convective storms. At the same time, decreasing trends emerge, especially at longer durations in Northern and Southern Italy and in parts of France. For RCP 4.5 projections, a similar pattern in the changes of the scale parameter is found (see Figure 10S in the Supplementary Material), with increasing trends at short durations in the Alpine Region and Central Italy and a general decreasing trend for longer durations.

The shape parameter at the beginning of the time series (1981), κ_1, has a clear pattern with latitude and orography (upper subplots in Fig. 4). In particular, at short durations there is a clear signature of orography, with the higher shape values (lighter distribution tails) located on the main mountainous regions (Alps and Apennines), in agreement with previous studies based on observations (Formetta et al., 2022; Marra et al., 2021). At longer durations, a positive dependence of the shape parameter with latitude also emerges, with higher shape at higher latitudes. This can be due to the greater intensity of more extreme events in the Mediterranean area (heavier distribution tails, smaller shape) and to a positive correlation between the shape parameter and the altitude, with greater values in the Apennines (Central Italy) and the Alps in the northern part (Northern Italy, Switzerland and Austria). Interestingly, the northern side of the Alps shows lower values of the shape parameter with respect to its southern side at all durations.

Maps in the lower subplots in Fig. 4 show the estimated slope (κ_2) of the shape parameter with time. Almost the entire domain is characterized by a negative trend (red areas), consistent with all three considered

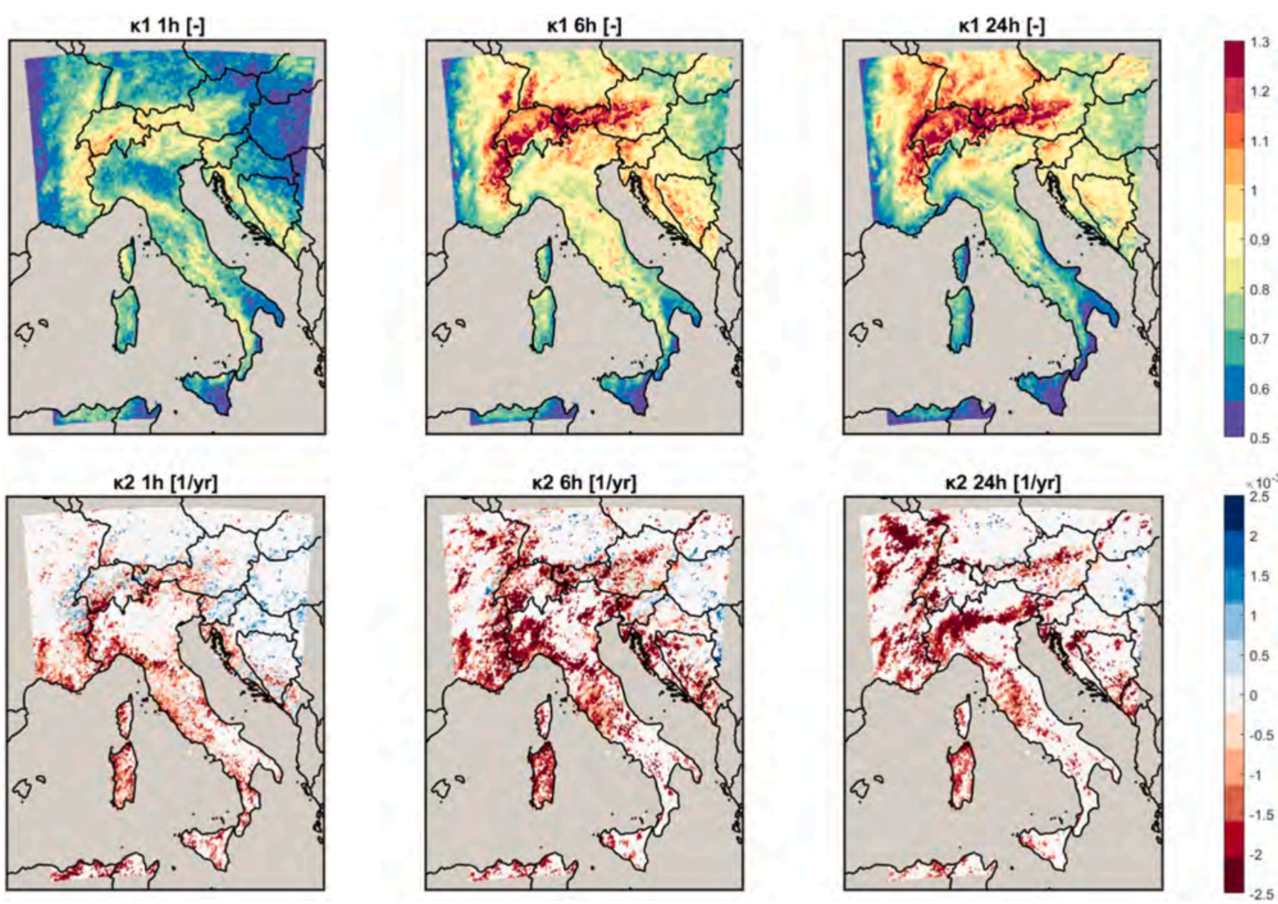

Fig. 4. Spatial map of κ_1, shape parameter at the beginning of the time series (1981), and κ_2, slope in the linear dependence over time for the RCP8.5 scenario. Grey areas represent the Mediterranean Sea or regions outside the VHR-PRO_IT domain.

durations. Positive changes are only visible in the northeastern part of the domain. This means that in most of the study region where non-stationarity is significant, the tail heaviness is projected to increase at all durations: larger extremes are expected to increase more than moderate extremes. This decrease in the shape parameter seems more relevant at the longer durations and, depending on duration, in some of the mountain regions, such as the Great Alpine area, Apennines, and Dinaric Alps in the east. An intensification of the most extreme events could be expected in the Alps in Northern Italy, Switzerland and the Southern part of Austria. Similar patterns are also found for the RCP 4.5 scenario (Figure 12S in the Supplementary Material), with a general negative trend of the shape parameter across the entire domain. Therefore, also in this scenario, an increase of the more extreme events is expected.

Fig. 5 shows the spatial median of the expected significant changes (% per decade) of the shape and scale parameters (according to Eq. (4) and Eq. (5)) across the entire domain. The median shape parameter (dashed lines) is projected to decrease for each duration and in both scenarios, with larger expected changes for longer durations. On the contrary, the scale parameter (solid lines) is projected to increase for short durations and to decrease for longer ones.

4.2. Expected changes in the precipitation quantiles

The trends in the distribution parameters (Figs. 3–5) can only suggest the direction of the changes in precipitation quantiles. In addition, some areas can experience possible compensation effects if there is a decrease of both the scale parameter (reduction of extreme events with all the return periods) and the shape parameter (increase of extreme events, especially with higher return periods), making the direction of changes uncertain. This is especially true for longer durations. Therefore, the actual trend signal in extreme precipitation can only be assessed by looking at the variation of the precipitation quantiles.

Fig. 6 shows the changes in extreme precipitation quantiles with return periods of 2 and 100 years in the areas in which the trend in the parameters of the fully non-stationary model (Eq. (3)) is statistically significant. White areas correspond to grid points where the null hypothesis of no trend (Eq. (1)) cannot be rejected or where changes in the extreme precipitation are close to zero.

The figures show a general increase in extreme precipitation quantiles (blue areas), especially in the Mediterranean area and the Alpine region at short durations. Particularly, positive changes are expected in central Italy, in Sardinia, and along the coast of Tuscany and Liguria for 1 h duration. Similar results are expected in the Alpine Region in Switzerland and Austria, and near the coast of Croatia, Bosnia and Montenegro for the same duration. On average, changes in the 100-year precipitation are greater than the ones expected for the 2-year rainfall, and this can be related to the expected decrease in the shape parameter in almost the whole domain. Some exceptions can be seen at shorter durations where the 2-year precipitation will increase more than the 100-year precipitation. For instance, this can be seen for the duration of 1 hour in Slovenia, where the 2–year precipitation is expected to increase for the positive changes in the scale parameter, and the 100-year precipitation will decrease due to increases of the shape parameter. Patchy patterns of reduction are present in the Eastern part of the domain, especially for shorter durations. Changes in extreme precipitation quantiles are referred to extreme precipitation with the same return periods at the beginning of the time series (1981), as shown in Figure 11S of the Supplementary Material. Additionally, the 10-year rainfall is included in the figure to qualitatively show the accuracy of the projections, as the maps fall within the same range as the 10-year rainfall from observations Poschlod et al. (2021) for different durations.

The changes in extreme precipitation in the RCP 4.5 have similar spatial patterns with the RCP 8.5 almost all over the domain (Figure 12S in the Supplementary Material), even if with slightly smaller expected changes. A difference can be found in northwestern Italy, as the RCP 4.5 shows that the hypothesis of a stationary model cannot be rejected, whereas an intensification of extreme precipitation is observed in the RCP 8.5.

Fig. 7 compares the spatial median across the entire domain of the expected changes of rare events (100-year return period events, solid lines) and more frequent ones (2-year events, dashed lines) for all the durations. Although the median changes are always positive for all considered quantiles, some differences emerge among 100-year and 2-year return period events, with the former (latter) increasing (decreasing) with duration. The median changes are about 3–4 % / decade at a 100-year return period and 2–3 % / decade at a 2-year return period. Greater changes are expected for rarer events as the tail heaviness is expected to increase (decreasing shape) for all the durations (red areas in Fig. 4), but especially for longer ones, where the change in the shape parameter is more relevant and compensates for the decreasing scale (Fig. 5). Moderate intense precipitation (2 years) will increase more at shorter durations, and these changes are likely related to the relevant increase of the scale parameter (Fig. 5). While greater values of change are expected for more extreme events at long durations, wider areas are interested by significant changes at short durations (right part of Fig. 7). It is worth noting the similar changes in the two scenarios (left part of Fig. 7 and Figure 19S in the Supplementary Material), and this is related to similar changes in the parameters distribution (Fig. 5), with slightly heavier tails in the RCP 4.5 that are compensated by higher changes in the scale in the RCP 8.5. However, less areas in the domain will have statistically significant trends in the RCP 4.5 (right part of Fig. 7).

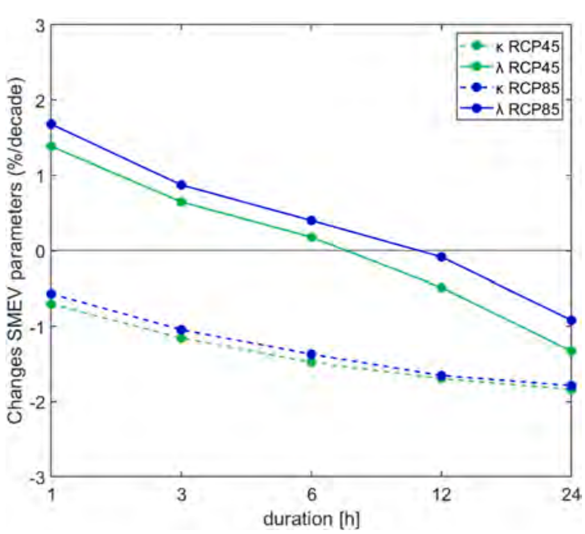

Fig. 5. Spatial median of significant changes in the SMEV parameters on a decadal basis (Eqs. (4) and 5). Solid lines represent the expected relative change of the scale parameter, while dashed lines refer to changes of the shape parameter. Green and blue colours are associated, respectively, with the RCP 4.5 and the RCP 8.5.

5. Discussion

Climate change will impact the frequency of extreme precipitation in central southern Europe, especially in the Mediterranean Area and the Alpine region. The results show a general increase of sub-daily precipitation in some regions of Italy, Switzerland, Austria and along the coast of the Mediterranean Sea in France, Slovenia, Croatia and Bosnia. There is a clear difference between the impact of climate change on extreme precipitation close to the Mediterranean Sea (generally clear patterns of increasing trends) and the northern part of the domain and Eastern Europe, with no expected changes or patchy patterns of decreasing trends. The changes reported for the RCP 4.5 scenario broadly agree with those for RCP 8.5 (Fig. 7 and Figure 19S in the Supplementary

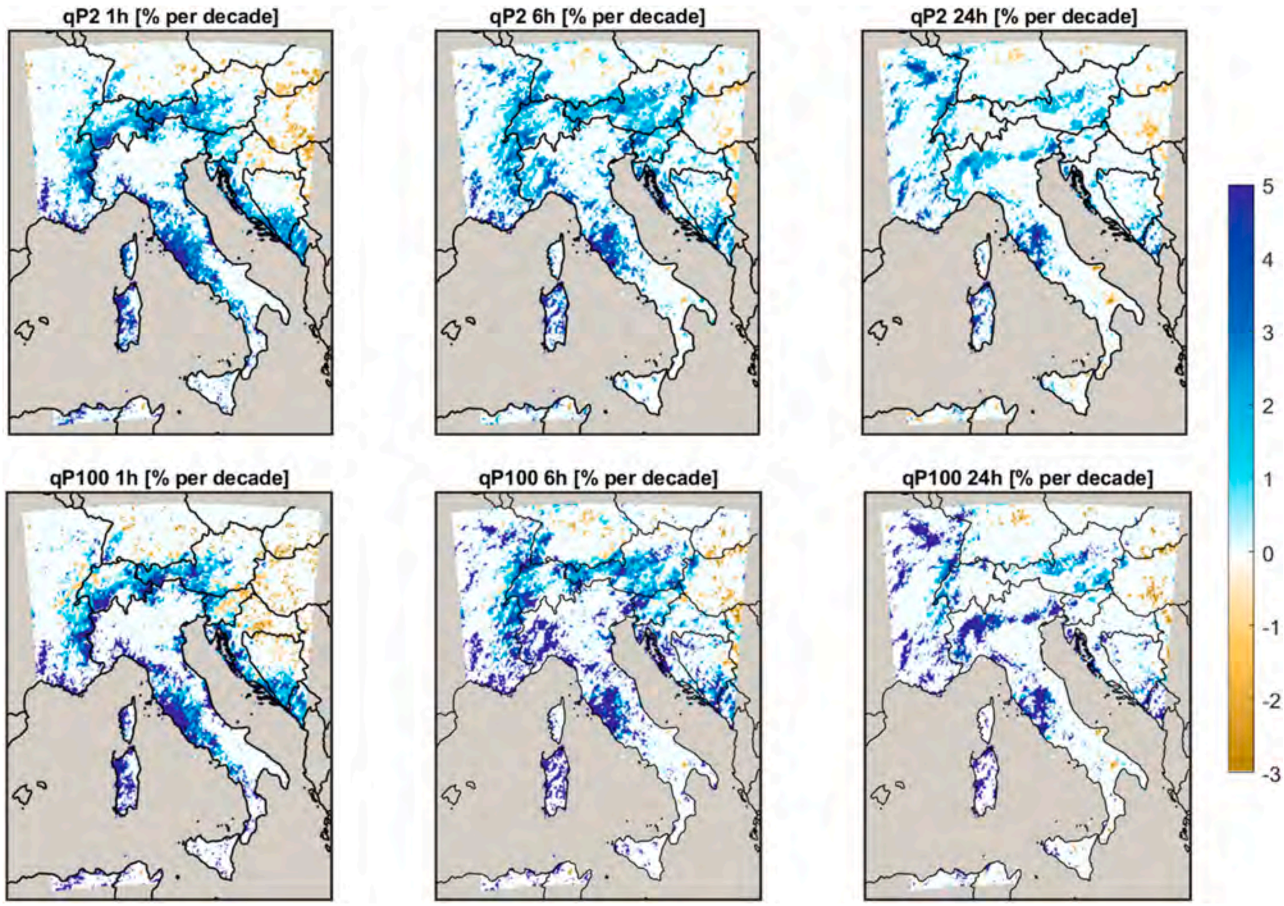

Fig. 6. Changes (% per decade) in 2y and 100y return period quantiles RCP 8.5, provided by the fully non-stationary model (Eq. (3)). An intensification of the extreme events is expected in the blue areas, while brown areas show a decreasing trend. White areas correspond to grid points where the stationary model cannot be rejected with a level of significance of 0.05 or where changes in the extreme precipitation are negligible. Grey areas represent the Mediterranean Sea or regions outside the VHR-PRO_IT domain.

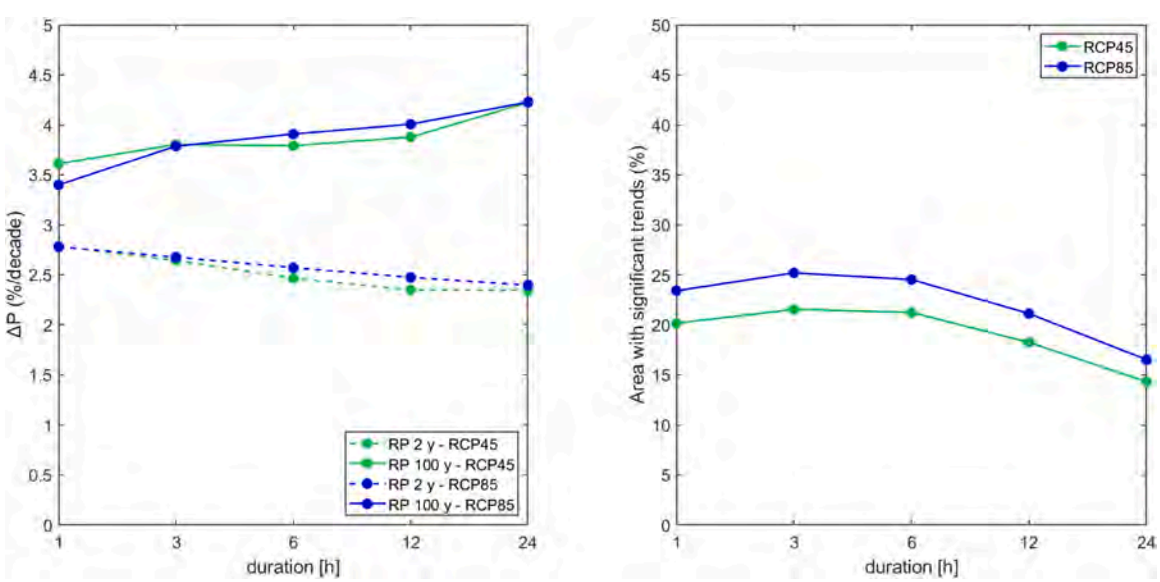

Fig. 7. Left part shows spatial median significant changes of 2y (dashed line) and 100y (solid line) return period (%/decade) based on RCP8.5 (blue) and RCP4.5 (green) scenarios. Right part shows the percentage of area with statistically significant changes for different durations and scenarios.

Material).

The intensification increases with the return period (Fig. 7), and this signal is related to statistically significant decreasing trends in the shape parameter (Figs. 2, 4, and 5). This result agrees with the findings of other studies based on the comparison between historical and future time windows (both assumed stationary), which found higher significant changes in rare extreme events compared to more frequent precipitation events (Butcher and Zi 2019; Cannon and Innocenti 2019; Dallan et al., 2024a,b; Gründemann et al., 2022; Hosseinzadehtalaei et al. 2020; Huo et al. 2021; Kharin et al. 2018; Li et al. 2021). The general reduction of the shape parameter, except for the northern part of the domain and Eastern Europe, is more relevant at longer durations and is associated with both increasing and decreasing trends in the scale parameter depending on the duration (Fig. 5). Indeed, over longer durations, many areas exhibit a 'compensation effect' between the two parameters, influencing changes in quantiles. A negative trend in the scale parameter reduces all extreme precipitation, while a negative trend in the shape parameter results in a heavier distribution tail, significantly increasing the most extreme events. This result explains why greater changes for the more extreme events are expected over longer durations, while shorter durations will see a higher increase in frequent extreme precipitation (Fig. 7). This occurs due to a combination of a significant rise in the scale parameter and a slight decrease in the shape parameter. Indeed, significant and positive changes in the scale parameters are associated with short durations in the Mediterranean areas (cyan areas in Fig. 2 and blue in Fig. 3, especially for 1 h). A possible interpretation of these results is that the changes in thermodynamic drivers (which are expected to mainly impact the scale parameter, see E. Dallan et al., 2024b) dominate at short durations, while changes induced by a combination of thermodynamic and large-scale dynamic drivers are to be expected at longer durations. This is not surprising as the increasing trend in short-duration precipitation extremes is likely induced by an intensification of convective precipitation (Dallan et al., 2022; Marra et al., 2024), while large-scale circulation is often important at longer-duration extremes (Andria et al. in review; Ciceri, 2024). For this reason, the results of the likelihood ratio test have shown more areas with statistically significant trends in the precipitation extremes at short durations (Fig. 6). Precipitation with a return period of 2 years will increase more at the shorter durations. Although based on different approaches, greater expected changes in the short-duration extreme precipitation with respect to the daily time scale have also been found in other works (Forestieri et al. 2018; Fowler et al. 2021a; Martel et al. 2020; Westra et al. 2014; Wood and Ludwig 2020). However, the more extreme precipitation (100 years) will increase more for longer durations for a significant decrease in the shape parameter. Changes in extreme precipitation in Southern and Northern Italy are associated with statistically significant changes in the shape parameter, while changes in extreme precipitation in Central Italy and Austria are due to statistically significant changes in the scale parameter (Fig. 2).

An interesting result consists of the agreement between the areas with statistically significant trends found in this study and Libertino et al. (2019) and Mazzoglio et al. (2025a), which perform a trend analysis over Italy based on rain gauge observations, highlighting regional patterns of positive or negative trends depending on the analyzed duration. The robust increase in precipitation extremes in central Italy and Southern France agrees with Caillaud et al. (2024), who found similar results analysing an ensemble of 13 CPM between 10-year historical and end-century periods under the RCP 8.5 scenario. Moreover, changes in extreme precipitation with short durations (Fig. 6) have a similar pattern to the results that Pichelli et al. (2021) obtained on the 99.9th summer hourly precipitation changes with an ensemble of 12 CPM projections. On the other hand, the results differ from the ones obtained in Raffa et al. (2023), who detected a reduction of the extreme precipitation in Southern Italy and the Islands. Nevertheless, even if the projections used in that study are the same, the authors considered the future changes in 2050 (instead of 2070) and the extreme precipitation as the 99.9th percentile of all the wet hours (which is almost 9 events per year, not nearly as extreme as the return levels investigated here). This comparison highlights the importance of assessing changes in extreme precipitation based on return periods to highlight possible increasing trends that are not detected with the percentiles. Indeed, Schär et al. (2016) demonstrated that wet-day percentiles are highly sensitive to changes in the frequency of wet days or hours, and can provide misleading interpretations when used to assess changes in heavy precipitation. The results of this study partially agree with E. Dallan et al. (2024b), who also found greater expected changes for the higher return periods. The results show the same trends in the Liguria and Tuscany regions, while some discrepancies are found in Northern Italy. Indeed, while the results of this work show an increase in extreme precipitation in Northwestern Italy, E. Dallan et al. (2024b) did not find the same trend in this region. However, the two studies considered different future time periods (2070 vs 2100) and climate projections (VHR-PRO_IT vs an ensemble of nine CPMs).

A limitation of this study is the consideration of a single climate model, which didn't allow us to assess the uncertainty related to the range of possible different future scenarios. However, not much can be done so far on this, as this is currently the only CPM covering southern central Europe with a long transient simulation. In addition, even if the linear dependence of the parameter on time seems a reasonable assumption (see Supplementary Material), more complex behaviors could better describe such dependence in the region, due to the interaction of multiple physical covariates (Andria et al., in review; Ciceri, 2024; Marra et al., 2024). Future studies could try to use non-stationary models linked to physical covariates.

However, the methodology presented in this study offers the possibility of detecting and explaining continuous change in extreme precipitation with remarkable accuracy, as the non-stationary frequency analysis conducted in this study avoids assuming stationarity in time slices and uses a model that has been proven to have greater fitting performances than both asymptotic and non-asymptotic competitors (Vidrio-Sahagún and He 2022). Therefore, this approach could be considered as a reference method to assess extreme precipitation changes when more long-transient CPM simulations will become available.

6. Conclusions

A non-stationary frequency analysis of convection permitting model projections over a 90 years for southern-central Europe has been conducted to assess the impact of climate change on sub-daily extreme precipitation quantiles in the area. To achieve this, we applied a non-stationary implementation of the SMEV model on VHR-PRO_IT projections, which is so far the only long transient CPM simulation in the study area. The projections are from the CMCC—CM Global Climate model with a downscaling at a convection-permitting scale of 2.2 km performed with the COSMO—CLM in two emission scenarios (RCP4.5 and RCP8.5). The non-stationary SMEV allows the use of a large set of ordinary events in the statistical inference, which can reduce sampling uncertainty compared to conventional approaches based on annual maxima, and permits a physical interpretation of the results. To the best of our knowledge, this represents the first attempt of a non-stationary and non-asymptotic frequency analysis on a long-term convection permitting model projection, and enabled us to describe the trend in extreme rainfall beyond the natural variability which could affect short (decadal) simulations.

In this approach, we use time as a covariate of our non-stationary model, as we are interested in describing the changes in the extremes over a long period with a transient climate. We assume that the two Weibull distribution parameters (scale and shape) change linearly over time. The accuracy of this approach could lead to this methodology being considered a reference for the analysis of long-term transient climate projections.

The results show areas in central southern Europe with a future intensification of the extreme precipitation. The expected changes are greater for rarer design events (median value of about 3–4 % / decade at 100 yr return period). Changes for short duration extremes are statistically significant in wider areas, but higher changes for long duration extremes emerge for higher return periods, related to statistically significant changes in the tail heaviness of their distribution. There is a clear difference between the expected changes obtained for the Alpine-Mediterranean areas (increasing trend) and the Eastern part of Europe (none or decreasing trend) for all the durations. These results suggest that changes in thermodynamic drivers, which primarily influence the scale parameter, dominate at short durations, while longer durations are affected by a combination of thermodynamic and large-scale dynamic drivers, influencing the shape parameter.

The changes reported for the RCP 4.5 scenario broadly agree with those for RCP 8.5, even if less widespread expected changes are shown for RCP 4.5.

The regions with a distinct climatic change signal in projected precipitation extremes identified here are broadly coherent with the observed trends in the study region. Hence, changes in precipitation intensities are already underway, lending credibility to these projections. Even though a limitation of this study is the consideration of a single climate model, which enables us to assess uncertainty, these results highlight the need to account for climate-induced changes in flood risk management and in the design of infrastructures.

Data statement

The climate projections used in this study (VHR-PRO_IT) are freely available at https://dds.cmcc.it/#/dataset/climate-projections-rcp85-downscaled-over-italy.

CRediT authorship contribution statement

Marco Lompi: Writing – original draft, Visualization, Software, Methodology, Investigation, Formal analysis, Data curation, Conceptualization. **Francesco Marra:** Writing – review & editing, Validation, Supervision, Software, Methodology, Investigation. **Roberto Deidda:** Writing – review & editing, Validation, Supervision, Investigation. **Enrica Caporali:** Writing – review & editing, Validation, Supervision, Investigation. **Marco Borga:** Writing – review & editing, Validation, Supervision, Methodology, Investigation, Conceptualization. **Eleonora Dallan:** Writing – review & editing, Visualization, Validation, Supervision, Software, Investigation, Data curation.

Declaration of competing interest

The authors declare that they have no known competing financial interests or personal relationships that could have appeared to influence the work reported in this paper.

Acknowledgements

Codes used for the study are freely available in public repositories: https://zenodo.org/records/14727998 (Marra, 2025).

The research is carried out within the RETURN – multi-Risk sciEnce for resilienT commUnities undeR a changiNg climate Extended Partnership and received funding from the European Union Next-GenerationEU (National Recovery and Resilience Plan – NRRP, Mission 4, Component 2, Investment 1.3 – D.D. 1243 2/8/2022, PE0000005). FM was supported by the INTENSE project (raINfall exTremEs and their impacts: from the local to the National ScalE) funded by the European Union - Next Generation EU in the framework of PRIN (Progetti di ricerca di Rilevante Interesse Nazionale) programme (Grant 2022ZC2522) and by the project "The Geosciences for Sustainable Development" (Budget Ministero dell'Università e della Ricerca–Dipartimenti di Eccellenza 2023–2027 C93C23002690001).

Supplementary materials

Supplementary material associated with this article can be found, in the online version, at doi:10.1016/j.advwatres.2025.105071.

References

Amponsah, W., Dallan, E., Nikolopoulos, E.I., Marra, F., 2022. Climatic and topographic controls on rainfall extremes and their temporal changes in data-sparse tropical regions. J. Hydrol. 612, 128090. https://doi.org/10.1016/j.jhydrol.2022.128090.

Andria, S., Borga, M., Marani, M. In review. "Thermodynamic vs. Large-scale controls on extreme precipitation: temporal scale dependence and Clausius-Clapeyron scaling redefined". ESS Open Arch.. January 11, https://doi.org/10.22541/essoar.173655785.54054918/v1.

Avanzi, F., De Michele, C., Gabriele, S., Ghezzi, A., Rosso, R., 2015. Orographic signature on extreme precipitation of short durations. J. Hydrometeorol. 16 (1), 278–294. https://doi.org/10.1016/j.advwatres.2021.104085.

Ban, N., Schmidli, J., Schär, C., 2014. Evaluation of the convection-resolving regional climate modeling approach in decade-long simulations. J. Geophys. Res. 119, 7889–7907. https://doi.org/10.1002/2014JD021478.

Ban, N., Rajczak, J., Schmidli, J., Schär, C., 2020. Analysis of Alpine precipitation extremes using generalized extreme value theory in convection-resolving climate simulations. Clim. Dyn. 55 (1), 61–75. https://doi.org/10.1007/s00382-018-4339-4, 86.

Ban, N., Caillaud, C., Coppola, E., Pichelli, E., Sobolowski, S., Adinolfi, M., Zander, M.J., 2021. The first multi-model ensemble of regional climate simulations at kilometer-scale resolution. Part I: evaluation of precipitation. Clim. Dyn. 57, 275–302. https://doi.org/10.1007/s00382-021-05708-w.

Butcher, J.B., Zi, T., 2019. Efficient method for updating IDF curves to future climate projections. Atmos. Ocean. Phys. https://doi.org/10.48550/arXiv.1906.04802.

Caillaud, C., Somot, S., Douville, H., Alias, A., Bastin, S., Brienen, S., Demory, M., Dobler, A., Feldmann, H., Frisius, T., Goergen, K., Kendon, E.J., Keuler, K., Lenderink, G., Mercogliano, P., Pichelli, E., Soares, P.M.M., Tölle, M.H., De Vries, H., 2024. Northwestern Mediterranean heavy precipitation events in a warmer climate: robust versus uncertain changes with a large convection-permitting model ensemble. Geophys. Res. Lett. 51, e2023GL105143. https://doi.org/10.1029/2023GL105143.

Caporali, E., Lompi, M., Pacetti, T., Chiarello, V., Fatichi, S., 2021. A review of studies on observed precipitation trends in Italy. Int. J. Clim. 41 (2021), E1–E25. https://doi.org/10.1002/joc.6741.

Cannon, A.J., Innocenti, S., 2019. Projected intensification of sub daily and daily rainfall extremes in convection-permitting climate model simulations over North America: implications for future intensity–duration–frequency curves. Nat. Hazards Earth Syst. Sci. 19 (2), 421–440. https://doi.org/10.5194/nhess-19-421-2019.

Chan, S.C., Kendon, E.J., Fowler, H.J., Youngman, B.D., Dale, M., Short, C., 2023. New extreme rainfall projections for improved climate resilience of urban drainage systems. Clim. V 30, 100375. https://doi.org/10.1016/j.cliser.2023.100375.

Ciceri R., 2024. "Thermodynamic and dynamic contributions to changes in extreme precipitation". https://thesis.unipd.it/handle/20.500.12608/80504.

Coles, S., 2001. An introduction to statistical modeling of extreme values. Springer Series in Statistics. Springer-Verlag, London. ISBN: 1-85233-459-2.

Dallan, E., Borga, M., Zaramella, M., Marra, F., 2022. Enhanced summer convection explains observed trends in extreme subdaily precipitation in the Eastern Italian Alps. Geophys. Res. Lett. 49, e2021GL096727. https://doi.org/10.1029/2021GL096727.

Dallan, E., Marra, F., Fosser, G., Marani, M., Formetta, G., Schär, C., Borga, M., 2023. How well does a convection-permitting regional climate model represent the reverse orographic effect of extreme hourly precipitation? Hydrol. Earth. Syst. Sci. 27, 1133–1149. https://doi.org/10.5194/hess-27-1133-2023, 2023.

Dallan, E., Borga, M., Fosser, G., Canale, A., Roghani, B., Marani, M., Marra, F., 2024a. A method to assess and explain changes in sub-daily precipitation return levels from convection-permitting simulations. Water. Resour. Res. 60 (5), e2023WR035969. https://doi.org/10.1029/2023WR035969.

Dallan, E., Marra, F., Fosser, G., Marani, M., Borga, M., 2024b. Dynamical factors heavily modulate the future increase of sub-daily extreme precipitation in the Alpine-Mediterranean region. Earth's Fut. 12, e2024EF005185. https://doi.org/10.1029/2024EF005185.

Donat, M.G., Lowry, A.L., Alexander, L.V., O'Gorman, P.A., Maher, N., 2016. More extreme precipitation in the world's dry and wet regions. Nat. Clim. Chang. 2016 (6), 508–513. https://doi.org/10.1038/nclimate2941.

Forestieri, A., Arnone, E., Blenkinsop, S., Candela, A., Fowler, H., Noto, L.V., 2018. The impact of climate change on extreme precipitation in Sicily, Italy. Hydrol. Process. 32 (3), 332–348. https://doi.org/10.1002/hyp.11421.

Formetta, G., Marra, F., Dallan, E., Zaramella, M., Borga, M., 2022. Differential orographic impact on sub-hourly, hourly, and daily extreme precipitation. Adv. Water. Resour. 149, 104085. https://doi.org/10.1016/j.advwatres.2021.104085.

Fosser, G., Kendon, E.J., Stephenson, D., Tucker, S., 2020. Convection-permitting models offer promise of more certain extreme rainfall projections. Geophys. Res. Lett. 47 (13), e2020GL088151. https://doi.org/10.1029/2020GL088151.

Fosser, G., Gaetani, M., Kendon, E.J., Adinolfi, M., Ban, N., Belušić, D., Caillaud, C., Careto, J.O.M., Coppola, E., Demory, M., de Vries, H., Dobler, A., Feldmann, H., Goergen, K., Lenderink, G., Pichelli, E., Schär, C., Soares, P.M.M., Somot, S., Tölle, M.H., 2024. Convection-permitting climate models offer more certain extreme rainfall projections. NPJ. Clim. Atmos. Sci. 7, 51. https://doi.org/10.1038/s41612-024-00600-w.

Fowler, H.J., Lenderink, G., Prein, A.F., Westra, S., Allan, R.P., Ban, N., Barbero, R., Berg, P., Blenkinsop, S., Do, H.X., Guerreiro, S., Haerter, J.O., Kendon, E.J., Lewis, E., Schaer, C., Sharma, A., Villarini, G., Wasko, C., Zhang, X., 2021a. Anthropogenic intensification of short-duration rainfall extremes. Nat. Rev. Earth Env. 2 (2), 107–122. https://doi.org/10.1038/s43017-020-00128-6.

Gründemann, G.J., van de Giesen, N., Brunner, L., van der Ent, R., 2022. Rarest rainfall events will see the greatest relative increase in magnitude under future climate

change. Commun. Earth Env. 3 (1), 235. https://doi.org/10.1038/s43247-022-00558-8.
Hosseini, S.R., Scaioni, M., Marani, M., 2020. Extreme Atlantic hurricane probability of occurrence through the metastatistical extreme value distribution. Geophys. Res. Lett. 47 (1), 2019GL086138. https://doi.org/10.1029/2019GL086138.
Hosseinzadehtalaei, P., Tabari, H., Willems, P., 2020. Climate change impact on short-duration extreme precipitation and intensity–duration–frequency curves over Europe. J. Hydrol. 590 (Nov), 125249. https://doi.org/10.1016/j.jhydrol.2020.125249.
Huo, R., Li, L., Chen, H., Xu, C.-Y., Chen, J., Guo, S., 2021. Extreme precipitation changes in Europe from the last millennium to the end of the twenty-first century. J. Clim 34 (2), 567–588. https://doi.org/10.1175/JCLI-D-19-0879.1.
IPCC, 2022. Climate Change 2022: impacts, adaptation, and vulnerability. In: Pörtner, H.-O., Roberts, D.C., Tignor, M., Poloczanska, E.S., Mintenbeck, K., Alegría, A., Craig, M., Langsdorf, S., Löschke, S., Möller, V., Okem, A., Rama, B. (Eds.), Contribution of Working Group II to the Sixth Assessment Report of the Intergovernmental Panel On Climate Change. Cambridge University Press. Cambridge University Press, Cambridge, UK and New York, NY, USA, p. 3056. https://doi.org/10.1017/9781009325844.
Kendon, E.J., Roberts, N.M., Fowler, H.J., Roberts, M.J., Chan, S.C., Senior, C.A., 2014. Heavier summer downpours with climate change revealed by weather forecast resolution model. Nat. Clim. Chang. 4 (7), 570–576. https://doi.org/10.1038/nclimate2258.
Kendon, E.J., Fischer, E.M., Short, C.J., 2023. Variability conceals emerging trend in 100yr projections of UK local hourly rainfall extremes. Nat. Commun. 14 (1), 1–14. https://doi.org/10.1038/s41467-023-36499-9.
Kharin, V.V., Flato, G.M., Zhang, X., Gillett, N.P., Zwiers, F., Anderson, K.J., 2018. Risks from climate extremes change differently from 1.5°C to 2.0°C depending on rarity. Earth's Fut. 6 (5), 704–715. https://doi.org/10.1002/2018EF000813.
Lee, O., Sim, I., Kim, S., 2020. Application of the non-stationary peak-over-threshold methods for deriving rainfall extremes from temperature projections. J. Hydrol. 585. https://doi.org/10.1016/j.jhydrol.2019.124318. Article 124318.
Li, C., Zwiers, F., Zhang, X., Chen, G., Lu, J., Li, G., Norris, J., Tan, Y., Sun, Y., Liu, M., 2019. Larger increases in more extreme local precipitation events as climate warms. Geophys. Res. Lett. 2019 46, 6885–6891. https://doi.org/10.1029/2019GL082908.
Li, C., Zwiers, F., Zhang, X., Li, G., Sun, Y., Wehner, M., 2021. Changes in annual extremes of daily temperature and precipitation in CMIP6 models. J. Clim 34 (9), 3441–3460. https://doi.org/10.1175/JCLI-D-19-1013.1.
Libertino, A., Ganora, D., Claps, P., 2019. Evidence for increasing rainfall extremes remains elusive at large spatial scales: the case of Italy. Geophys. Res. Lett. 2019 46, 7437–7446. https://doi.org/10.1029/2019GL083371.
Lompi, M., Mediero, L., Soriano, E., Caporali, E., 2023. Climate change and hydrological dam safety: a stochastic methodology based on climate projections. Hydrol. Sci. J. 68, 745–763. https://doi.org/10.1080/02626667.2023.2192873.
Lucas-Picher, P., Argüeso, D., Brisson, E., Tramblay, Y., Berg, P., Lemonsu, A., Kotlarski, S., Caillaud, C., 2021. Convection-permitting modeling with regional climate models: latest developments and next steps. WIREs Clim. Change 12 (6), e731. https://doi.org/10.1002/wcc.731.
Luu, L.N., Vautard, R., Yiou, P., Soubeyroux, J.-M., 2022. Evaluation of convection-permitting extreme precipitation simulations for the south of France. Earth Syst. Dynam. 13, 687–702. https://doi.org/10.5194/esd-13-687-2022.
Marani, M., Ignaccolo, M., 2015. A metastatistical approach to rainfall extremes. Adv. Water. Resour. 79, 121–126. https://doi.org/10.1016/j.advwatres.2015.03.001.
Marra, F., Zoccatelli, D., Armon, M., Morin, E., 2019. A simplified MEV formulation to model extremes emerging from multiple nonstationary underlying processes. Adv. Water. Resour. 127, 280–290. https://doi.org/10.1016/j.advwatres.2019.04.002.
Marra, F., Borga, M., Morin, E., 2020. A unified framework for extreme subdaily precipitation frequency analyses based on ordinary events. Geophys. Res. Lett. 47 (18), e2020GL090209. https://doi.org/10.1029/2020gl090209.
Marra, F., Armon, M., Borga, M., Morin, M., 2021. Orographic effect on extreme precipitation statistics peaks at hourly time scales. Geophys. Res. Lett., e2020GL091498 https://doi.org/10.1029/2020GL091498.
Marra, F., Armon, M., Morin, E., 2022. Coastal and orographic effects on extreme precipitation revealed by weather radar observations. Hydrol. Earth. Syst. Sci. 26, 1439–1458. https://doi.org/10.5194/hess-26-1439-2022.
Marra, F., Koukoula, M., Canale, A., Peleg, N., 2024. Predicting extreme sub-hourly precipitation intensification based on temperature shifts. Hydrol. Earth. Syst. Sci. 28, 375–389. https://doi.org/10.5194/hess-28-375-2024.
Marra, F., 2025. Nonstationary SMEV model (MLE parameter estimation with left-censoring for the two-parameter Weibull distribution). Zenodo. https://doi.org/10.5281/zenodo.14727998.
Martel, J.-L., Mailhot, A., Brissette, F., 2020. Global and regional projected changes in 100-yr subdaily, daily, and multiday precipitation extremes estimated from three large ensembles of climate simulations. J. Clim. 33, 1089–1103. https://doi.org/10.1175/JCLI-D-18-0764.1.
Martel, J.-L., Brissette, F., Lucas-Picher, P., Troin, M., Arsenault, R., 2021. Climate change and rainfall intensity–duration–frequency (IDF) curves: overview of science and guidelines for adaptation. J. Hydrol. Eng. https://doi.org/10.1061/(ASCE)HE.1943-5584.000212.
Mazzoglio, P., Butera, I., Claps, P., 2020. I2-RED: a massive update and quality control of the Italian annual extreme rainfall dataset. Water. (Basel) 12, 3308. https://doi.org/10.3390/w12123308.
Mazzoglio, P., Viglione, A., Ganora, D., Claps, P., 2025a. Mapping the uneven temporal changes in ordinary and extraordinary rainfall extremes in Italy. J. Hydrol.: Reg. Stud. 58 (102287). https://doi.org/10.1016/j.ejrh.2025.102287.
Mazzoglio, P., Lompi, M., Marra, F., Dallan, E., Deidda, R., Claps, P., Manfreda, S., Noto, L.V., VIglione, A., Raffa, M., Mercogliano, P., Marani, M., Caporali, E., Borga, M., 2025b. Orographic and sea-land contrast effects in convection-permitting simulations of extreme sub-daily precipitation. Weather. Clim. Extrem., 100798 https://doi.org/10.1016/j.wace.2025.100798.
Meredith, E.P., Ulbrich, U., Rust, H.W., 2020. Subhourly rainfall in a convection-permitting model. Environ. Res. Lett. 15 (3), 034031. https://doi.org/10.1088/1748-9326/ab6787.
Miniussi, A., Marani, M., G Villarini, G., 2020a. Metastatistical extreme value distribution applied to floods across the continental United States. Adv. Water. Resour. 136, 103498. https://doi.org/10.1016/j.advwatres.2019.103498.
Miniussi, A., Villarini, G., Marani, M., 2020b. Analyses through the metastatistical extreme value distribution identify contributions of tropical cyclones to rainfall extremes in the eastern United States. Geophys. Res. Lett. 47 (7), e2020GL087238. https://doi.org/10.1029/2020gl087238.
Munich *Re*: Flood risks on the rise. https://www.munichre.com/en/risks/natural-disasters/1015floods.html. Accessed 30 October 2023 (2023).
Overeem, A., Buishand, T.A., Holleman, I., 2008. Rainfall depth–Duration–Frequency curves and their uncertainties. J. Hydrol. 348, 124–134. https://doi.org/10.1016/j.jhydrol.2007.09.044.
Panziera, L., Gabella, M., Zanini, S., Hering, A., Germann, U., Berne, A., 2016. A radar-based regional extreme rainfall analysis to derive the thresholds for a novel automatic alert system in Switzerland. Hydrol. Earth. Syst. Sci. 20, 2317–2332. https://doi.org/10.5194/hess-20-2317-2016.
Papalexiou, S.M., Montanari, A., 2019. Global and regional increase of precipitation extremes under global warming. Water. Resour. Res. 55, 4901–4914. https://doi.org/10.1029/2018WR024067.
Pichelli, E., Coppola, E., Sobolowski, S., Ban, N., Giorgi, F., Stocchi, P., Vergara-Temprado, J., 2021. The first multi-model ensemble of regional climate simulations at kilometer-scale resolution. Part 2: historical and future simulations of precipitation. Clim. Dyn. 56, 3581–3602. https://doi.org/10.1007/s00382-021-05657-4.
Poschlod, B., Ludwig, R., Sillmann, J., 2021. Ten-year return levels of sub-daily extreme precipitation over Europe. Earth. Syst. Sci. Data 13, 983–1003. https://doi.org/10.5194/essd-13-983-2021.
Prein, A.F., Langhans, W., Fosser, G., Ferrone, A., Ban, N., Goergen, K., Keller, M., Tölle, M., Gutjahr, O., Feser, F., et al., 2015. A review on regional convection-permitting climate modeling: demonstrations, prospects, and challenges. Rev. Geophys. 53, 323–361. https://doi.org/10.1002/2014RG000475.
Prein, A.F., Rasmussen, R.M., Ikeda, K., Liu, C., Clark, M.P., Holland, G.J., 2017. The future intensification of hourly precipitation extremes. Nat. Clim. Chang. 7, 48–52. https://doi.org/10.1038/nclimate3168.
Prosdocimi, I., Kjeldsen, T., 2021. Parametrisation of change-permitting extreme value models and its impact on the description of change. Stoch. Env. Res. Risk. Assess 35, 307–324. https://doi.org/10.1007/s00477-020-01940-8.
Rashid, M.M., Beecham, S., Chowdhury, R.K., 2017. Simulation of extreme rainfall and projection of future changes using the GLIMCLIM model. Theor. Appl. Clim. 130, 453–466. https://doi.org/10.1007/s00704-016-1892-9.
Raffa, M., Adinolfi, M., Reder, A., Marras, G.F., Mancini, M., Scipione, G., Santini, M., Mercogliano, P., 2023. Very high resolution projections over Italy under different CMIP5 IPCC scenarios. Sci. Data 10, 238. https://doi.org/10.1038/s41597-023-02144-9.
Schär, C., Ban, N., Fischer, E.M., Rajczak, J., Schmidli, J., Frei, C., Giorgi, F., Karl, T.R., Kendon, E.J., Tank, A.M.G.K., O'Gorman, P.A., Sillmann, J., Zhang, X., Zwiers, F.W., 2016. Percentile indices for assessing changes in heavy precipitation events. Clim. Change 137 (1), 201–216. https://doi.org/10.1007/s10584-016-1669-2.
Seo, J., Won, J., Choi, J., Lee, J., Jang, S., Lee, O., Kim, S., 2021. Uncertainty of rate of change in Korean future rainfall extremes using non-stationary GEV model. Atmosphere 12 (2), 227. https://doi.org/10.3390/atmos12020227.
(Chapter 11) Seneviratne, S.I., Zhang, X., Adnan, M., Badi, W., Dereczynski, C., Di Luca, A., Ghosh, S., Iskander, I., Kossin, J., Lewis, S., Otto, F., Pinto, I., Satoh, M., Vicente-Serrano, S.M., Wehner, M., Zhou, B., et al., 2021. Weather and climate extreme events in a changing climate (Chapter 11). In: Masson-Delmotte, V., Zhai, P., Pirani, A., Connors, S.L., Péan, C., Berger, S., Caud, N., Chen, Y., et al. (Eds.), IPCC 2021: Climate Change 2021: The Physical Science Basis. Contribution of Working Group I to the Sixth Assessment Report of the Intergovernmental Panel On Climate Change. Cambridge University Press, Cambridge, United Kingdom and New York, NY, USA, pp. 1513–1766. https://doi.org/10.1017/9781009157896.013.
Siena, M., Levizzani, V., Marra, F., 2023. A method to derive satellite-based extreme precipitation return levels in poorly gauged areas. J. Hydrol. 626, 130295. https://doi.org/10.1016/j.jhydrol.2023.130295.
Silva, D.F., Simonovic, S., Schardong, A., Goldenfum, J.A., 2021. Introducing non-stationarity into the development of intensity-duration-frequency curves under a changing climate. Water 13 (8), 1008. https://doi.org/10.3390/w13081008.
Sojan, J.M., Srivastav, R., Meghana, N., 2023. Regional non-stationary future extreme rainfall under changing climate over Asian monsoon region. Atmos. Res. 284, 106592. https://doi.org/10.1016/j.atmosres.2022.106592.
Vidrio-Sahagun, C.T., He, J., 2022. Hydrological frequency analysis under nonstationarity using the metastatistical approach and its simplified version. J. Hydrol 16. https://doi.org/10.1016/j.advwatres.2022.104244. Article 104244.
Westra, S., Fowler, H.J., Evans, J.P., Alexander, L.V., Berg, P., Johnson, F., Kendon, E.J., Lenderink, G., Roberts, N.M., 2014. Future changes to the intensity and frequency of short-duration extreme rainfall. Rev. Geophys. 52, 522–555. https://doi.org/10.1002/2014RG000464.
Wilson, P.S., Toumi, R., 2005. A fundamental probability distribution for heavy rainfall. Geophys. Res. Lett. 32 (14). https://doi.org/10.1029/2005GL022465.

Wood, R.R., Ludwig, R., 2020. Analyzing internal variability and forced response of subdaily and daily extreme precipitation over Europe. Geophys. Res. Lett. 47 (17), e2020GL089300. https://doi.org/10.1029/2020GL089300.

Zhang, W., Zhou, T., Wu, P., 2024. Anthropogenic amplification of precipitation variability over the past century. Science 385 (6707), 427–432. https://doi.org/10.1126/science.adp0212.

Zorzetto, E., Botter, G., Marani, M., 2016. On the emergence of rainfall extremes from ordinary events. Geophys. Res. Lett. 43 (2016), 8076–8082. https://doi.org/10.1002/2016GL069445.